
# Reconfigurable Intelligent Surface-assisted Secure Mobile Edge Computing Networks

| | |
|---|---|
| Journal: | *IEEE Transactions on Vehicular Technology* |
| Manuscript ID | VT-2021-03587 |
| Suggested Category: | Regular Paper |
| Date Submitted by the Author: | 08-Oct-2021 |
| Complete List of Authors: | Mao, Sun; Sichuan Normal University, College of Computer Science<br>Liu, Lei; Xidian University, State Key Laboratory of Integrated Service Networks<br>Zhang, Ning; University of Windsor,<br>Dong, Mianxiong; Muroran Institute of Technology, Department of Information and Electronic Engineering<br>Zhao, Jun; Nanyang Technological University, School of Computer Engineering<br>Wu, Jinsong; Universidad de Chile, Department of Electrical Engineering<br>Leung, Victor; Shenzhen University, College of Computer and Software Engineering; The University of British Columbia, Department of Electrical and Computer Engineering |
| Keywords: | Mobile edge computing, reconfigurable intelligent surface, computation efficiency, Security |
| | |

# Reconfigurable Intelligent Surface-assisted Secure Mobile Edge Computing Networks

Sun Mao, Lei Liu, Ning Zhang, Mianxiong Dong, Jun Zhao, Jinsong Wu, and Victor C. M. Leung

***Abstract*—Mobile edge computing (MEC) has been recognized as a viable technology to satisfy low-delay computation requirements for resource-constrained Internet of things (IoT) devices. Nevertheless, the broadcast feature of wireless electromagnetic communications may lead to the security threats to IoT devices. In order to enhance the task offloading security, this paper proposes a reconfigurable intelligent surface (RIS)-assisted secure MEC network framework. Furthermore, we investigate the max-min computation efficiency problem under the secure computation rate requirements, by jointly optimizing the local computing frequencies and transmission power of IoT devices, time-slot assignment, and phase beamforming of the RIS. To solve the formulated non-convex problem, we further develop an iterative algorithm, in which the Dinkelbach-type method and block coordinate descent (BCD) technique are utilized to tackle the fractional objective function and coupled optimization variables, respectively. In particular, the successive convex approximation (SCA) and penalty function-based methods are exploited to solve the transmit power control and reflecting beamforming optimization subproblems, respectively, and the closed-form expression for local computing frequencies optimization subproblem is derived. Numerical results quantify the performance gain achieved by the proposed RIS-assisted secure MEC networks, when compared to existing benchmark methods.**

***Index Terms*—Mobile edge computing, reconfigurable intelligent surface, computation efficiency, security.**

## I. Introduction

### A. Motivation and Scope

In recent years, the rapid penetrations of Internet of things (IoTs) have motivated a variety of computation-intensive and delay-sensitive mobile applications, such as intelligent transportation systems, smart city, and so forth, which impose great pressures on size- and resource-constrained IoT devices [1], [2]. Therefore, mobile edge computing (MEC) has been proposed a viable design paradigm to tackle this issue by allowing the computation offloading from IoT devices to access points (APs) integrated with edge servers [3], [4]. Benefitting from deploying edge servers close to IoT devices, MEC is able to reduce the transmission delay and energy consumption during the task offloading process, as compared to the centralized cloud computing architecture.

Despite the benefits brought by MEC, the wireless task offloading also introduces severe security challenges. Since the broadcast feature of wireless electromagnetic communications, the computation tasks offloaded from IoT devices to the AP may be overheard by nearby eavesdroppers, which will lead to the security threats to IoT devices [5], [6]. The physical layer security (PLS) technique is a promising method to ensure the security of task offloading in MEC networks. Nevertheless, in order to achieve the high-efficient utilization of PLS technique, the channel gains of legitimate links should be better than that of the eavesdropping link, which not always holds.

On the other hand, reconfigurable intelligent surface (RIS) has been envisioned as a key technique in the future sixth-generation (6G) mobile communication systems, due to its ability to actively customize wireless propagation environments [7], [8]. In particular, RIS is a panel integrated with a large number of passive reflection elements, which can achieve fine-grained reflect beamforming for enhancing the signal strength at legitimate receivers and avoiding information leakage to malicious eavesdroppers, by adjusting the phases of incident signals [9], [10]. Therefore, integrated RIS with PLS technique has great potential to achieve secure task offloading in MEC networks. Furthermore, the computation efficiency defined as computation-bits-per-joule, is envisioned as an important performance metric to balance the computation capability and energy consumption [11], [12]. Therefore, this paper focuses on investigating the secure task offloading and wireless resource management strategy for RIS-assisted MEC networks, in order to maximize the user computation efficiency, and meanwhile ensuring the secure computation rate requirements of IoT devices.

### B. Related Works

We summarize the related works by concentrating on (i) Task offloading in mobile edge computing, (ii) Security in mobile edge computing, (iii) RIS-enhanced secure communications.

*1) Task Offloading in Mobile Edge Computing:* In MEC, there usually exists two types of offloading modes, i.e., the

Sun Mao is with College of Computer Science, Sichuan Normal University, Chengdu, 610101, China. (E-mail: sunmao@sicnu.edu.cn).

Lei Liu is with the State Key Laboratory of Integrated Service Networks, Xidian University, Xian 710071, China (E-mail: tianjiaoliulei@163.com).

Ning Zhang is with the Department of Electrical and Computer Engineering, University of Windsor, ON, N9B 3P4, Canada (E-mail: ning.zhang@ieee.org).

Mianxiong Dong is with the Department of Sciences and Informatics, Muroran Institute of Technology, Muroran 050-8585, Japan (e-mail: mx.dong@csse.muroran-it.ac.jp).

Jun Zhao is with the School of Computer Science and Engineering, Nanyang Technological University, Singapore (E-mail: junzhao@ntu.edu.sg).

Jinsong Wu is with Department of Electrical Engineering, Universidad de Chile, Santiago, Chile (E-mail: wujs@ieee.org).

Victor C. M. Leung is with Shenzhen University, Shenzhen, China and the University of British Columbia, Vancouver, Canada (E-mail: vleung@ieee.org).

binary offloading mode and the partial offloading mode. In the former scheme, the computation task can only be executed either locally or completely offloaded to an edge node as a whole. In [13], Bi *et. al* aimed at maximizing total computation bits for wireless powered MEC networks with the binary offloading strategy. The same group extended this work to the scenario considering the stochastic channel states and task arrivals in [14]. They further proposed an intelligent task offloading method by exploiting the deep reinforcement learning technique. For the partial offloading scheme, the task is able to be arbitrarily partitioned for locally computing and remotely executing at the MEC server in parallel. In [15], You *et. al* studied energy-efficient resource allocation strategy for an MEC network with partial offloading. [16] and [17] adopted the non-orthogonal multiple access (NOMA) and RIS techniques to improve the task offloading efficiency, respectively. Accounting for the limited computing capability at MEC server, [18] put forward a cooperative communication and computation resources sharing mechanism among IoT devices, in order to satisfy massive computing requirements in the future IoTs.

*2) Security in Mobile Edge Computing:* Despite the low-delay computation experiences brought by the MEC architecture, however, the offloading data may be intercepted and overheard by nearby eavesdroppers, due to the broadcast nature of electromagnetic signals. Therefore, it is essential to design secure task offloading scheme for avoiding information leakage. In [19], Wang *et. al* considered a multi-user MEC network with malicious eavesdroppers. In addition, they further proposed an approach to minimize the system energy consumption, under the computing delay and secure offloading constraints. In [20], [21], the authors utilized the secrecy outage probability to measure the task offloading performance, with the assumption of knowing the distribution of eavesdropped channels. Based on this indicator, the total energy consumption was optimized for unmanned aerial vehicle-enabled MEC networks and NOMA-enabled MEC networks, respectively.

*3) RIS-enhanced secure communications:* Due to the reflection beamforming gain brought by RIS, a variety of research works investigated the RIS-enhanced secure communications. In [22], Chen *et. al* first proposed to utilize RIS to improve the physical layer security communications. They further developed a joint transmit beamforming and reflecting beamforming method to maximize the minimum secrecy rate. In [23], Hong *et. al* considered an artificial noise (AN)-enhanced multiple-input-multiple-output communication systems assisted by the RIS. To maximize the secure rate, they developed an approach to jointly optimize the transmit precoding matrix of AP, covariance matrix of AN and phase beamforming at the RIS. Above works generally supposed that the AP can obtain perfect channel state information (CSI). However, potential eavesdroppers are inclined to hide their locations, so it is challenging to obtain the CSI of eavesdropping channels. Therefore, Yu *et. al* in [24] investigated the sum rate maximization problem for RIS-assisted secure communication systems, considering the imperfect CSI of the eavesdropper channels. Moreover, Xu *et. al* in [25] focused on minimizing the eavesdropped information amount while ensuring the secure communication requirements.

From above descriptions, it should be noted that the design problem for RIS-assisted MEC networks against malicious eavesdroppers has yet been investigated. Specifically, it is essential to ensure the security of task offloading in MEC networks. These observations motivate us to develop the RIS-assisted secure computation offloading and resource management mechanism for MEC networks.

### C. Contributions and Organizations

The main contribution of this paper is to design a secure computation offloading strategy for RIS-assisted MEC networks, detailed as follows.

- Different from the existing works about task offloading security in MEC networks [19], [20], [21], this paper presents a RIS-assisted secure MEC network framework, where the RIS is properly deployed and utilized to assist the task offloading from IoT devices to the AP, and meanwhile avoiding the information leakage to malicious eavesdroppers.
- In order to investigate RIS-assisted secure task offloading, we establish a joint optimization of time-slot assignment, phase beamforming of RIS, local computing frequencies and transmit power of IoT devices, with the objective of max-min computation efficiency, while satisfying the secure computation rate requirements of IoT devices.
- To solve the formulated non-convex non-linear optimization problem, we first employ the Dinkelbach-type method and block coordinate descent algorithm to transform the original problem to several subproblems, namely transmit power control, time-slot assignment, phase beamforming design, and local computing frequencies optimization subproblems. In particular, the successive convex approximation-based method and penalty function-based method are established to solve the transmit power control and phase beamforming optimization subproblems, respectively, and the closed-from expressions are derived for the local computing frequencies optimization subproblem.

The remainder of this paper is organized as follows. Section II introduces the system model of RIS-assisted MEC networks. Section III establishes the max-min computation energy efficiency problem, and presents the proposed optimization algorithm. Section IV provides simulation results to validate the performance of the proposed method. Section V concludes this paper.

## II. System Model

As illustrated in Fig. 1, this paper considers a RIS-assisted MEC network composed of an access point (AP) equipped with the edge computing server, a RIS with $M$ reflection elements, $K$ IoT devices, and a malicious eavesdropper. The IoT devices and reflection elements are indexed by $\mathcal{K} \in \{1, 2, \cdots, K\}$ and $\mathcal{M} = \{1, 2, \cdots, M\}$, respectively. In addition, we supposed that all wireless terminals are equipped

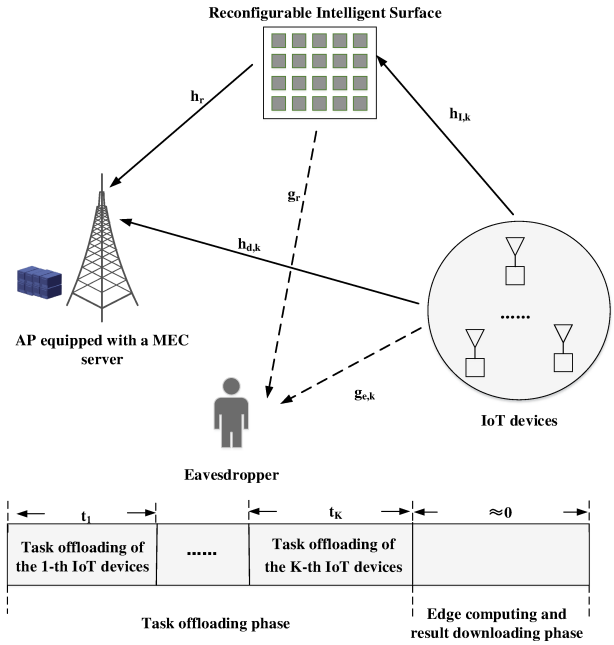


**Fig. 1:** RIS-assisted MEC with an eavesdropper.

**TABLE I:** Summary of Key Notations

| Notation | Description |
|---|---|
| $K$ | Number of IoT devices |
| $T$ | Time block length |
| $M$ | Number of reflection units at RIS |
| $W$ | System total bandwidth |
| $\kappa$ | Effective capacitance factor |
| $D_{L,k}$ | Local computing bits of $k$-th IoT device |
| $D_{O,k}$ | Secure offloading throughput of $k$-th IoT device |
| $f_k$ | Local computing frequency of $k$-th IoT device |
| $C_k$ | Task complexity of $k$-th IoT device |
| $t_k$ | Offloading time slot assigned to $k$-th IoT device |
| $p_k$ | Transmit power of $k$-th IoT device |
| $\Delta_k$ | Phase beamforming matrix of RIS during $t_k$ |
| $N_0$ | Gaussian noise power |
| $D_k$ | Size of total accomplished tasks of $k$-th IoT device |
| $E_k$ | Total energy consumption of $k$-th IoT device |
| $\eta_{\mathrm{EE},k}$ | Computation energy efficiency of $k$-th IoT device |

with a single antenna. Benefiting from the novel paradigm of partial offloading mode in MEC, the IoT device can transmit part of its computation tasks to the AP with the aid of RIS. Due to the broadcast nature of wireless electromagnetic waves, an eavesdropper located within the MEC network can intentionally overhear the offloaded data from IoT devices. For the purpose of ensuring the security during the task offloading process, this paper proposes to utilize the RIS and physical layer security techniques to avoid the information leakage to the malicious node. The main symbols adopted in this work are illustrated in TABLE I for ease reference.

It should be noted that our considered system can be found in practical application scenario. Taking a wireless camera for example, these IoT devices are deployed to execute some monitor tasks, e.g., environmental surveillance, target recognition, and so forth. In order to achieve the real-time video analysis, the resource-constrained wireless cameras must offload part of their raw data to nearby AP for remote analysising. Nonetheless, there exists some malicious eavesdroppers which are interested in the collected data by wireless cameras, so the eavesdroppers are intent to overhear the wireless cameras' offloaded raw data.

### A. Channel Model

The channel coefficients from the $k$-th IoT device to the AP, from the $k$-th IoT device to the RIS, from the RIS to the AP, from the $k$-th IoT device to the eavesdropper, and from the RIS to the eavesdropper are denoted by $h_{d,k}$, $\mathbf{h}_{I,k} \in \mathbb{C}^{M\times 1}$, $\mathbf{h}_r^H \in \mathbb{C}^{1\times M}$, $g_{e,k}$, and $\mathbf{g}_r^H \in \mathbb{C}^{1\times M}$, respectively. Suppose that all the channels follow block-based fading, i.e., the channels remain constant during the current time block but may change over different time blocks. Similar to [22], [23], we suppose that the AP can acquire perfect CSI of all channels. Then, the AP will perform resource management strategy to maximize the computation efficiency of IoT devices. Although the assumption of perfect CSI is ideal, the method proposed in this paper allows us to reveal the performance upper bound of considered RIS-assisted MEC networks.

### B. Local Computing

The IoT devices will process part of their computation tasks via local central processing unit (CPU) during the entire time block. Therefore, the number of locally accomplished tasks of the $k$-th IoT device and the computing energy consumption are given by

$$D_{L,k} = \frac{f_k T}{C_k} \tag{1}$$

and

$$E_{L,k} = \kappa f_k^3 T, \tag{2}$$

respectively, where $f_k$ denotes the CPU cycle of the $k$-th IoT device, $T$ stands for the time slot length, $C_k$ represents the computational complexity, and $\kappa$ is the effective capacitance factor [3].

### C. Security-driven Task Offloading

As illustrated in Fig. 1, the IoT devices transmit part of their computation tasks to the AP in a time-division manner. In addition, the physical layer security technique will be utilized to avoid the data leakage to the eavesdropper. The secure offloading rate from the $k$-th IoT device to the AP will be

$$\begin{aligned} D_{S,k} =& [t_k W \log_2\left(1+\frac{p_k|\mathbf{h}_r^H\Delta_k\mathbf{h}_{I,k}+h_{d,k}|^2}{N_0}\right) - \\ & t_k W \log_2\left(1+\frac{p_k|\mathbf{g}_r^H\Delta_k\mathbf{h}_{I,k}+g_{d,k}|^2}{N_0}\right)]^+, \end{aligned} \tag{3}$$

where $[x]^+ = \max\{x, 0\}$, $t_k$ and $p_k$ denote the sub-slot duration and the transmission power of the $k$-th IoT device, respectively, $W$ represents the system bandwidth, $N_0$ is the Gaussian noise power, and $\Delta_k = \text{diag}\{e^{j\phi_{k,1}}, \cdots, e^{j\phi_{k,M}}\}$, where $j$ stands for the imaginary unit, and $\phi_{k,m} \in [0, 2\pi]$ represents the phase shift of $m$-th passive element during $t_k$.

After receiving the computation tasks of IoT devices, the MEC server located at AP will process the received computation tasks and transmit the corresponding computing results to IoT devices. Because the MEC server has powerful computing capacity and the size of computing results is small [26], [27], we ignore the process of edge computing and result returning in this work.

### D. Computation Energy Efficiency

The total accomplished computation task of the $k$-th IoT device during the current time block is the sum of locally computed bits and offloaded bits, i.e.,

$$D_k = D_{L,k} + D_{S,k}. \tag{4}$$

Meanwhile, the energy consumption of the $k$-th IoT device will be

$$E_k = p_k t_k + E_{L,k}, \tag{5}$$

where the first term in the right side of (5) stands for the transmission energy consumption of the $k$-th IoT device. Therefore, the computation energy efficiency of $k$-th IoT device is defined as the ratio of $D_k$ to $E_k$, i.e.,

$$\eta_{\text{EE},k} = \frac{D_k}{E_k}. \tag{6}$$

## III. Max-Min Computation Efficiency Optimization Problem

Based on above descriptions, we formulate a max-min computation energy efficiency problem under the secure computation rate constraints of IoT devices, with the joint optimization of time-slot assignment $\{t_k, \forall k \in \mathcal{K}\}$, passive beamforming $\{\Delta_k, \forall k \in \mathcal{K}\}$ of the RIS, transmit power $\{p_k, \forall k \in \mathcal{K}\}$ and local computing frequencies $\{f_k, \forall k \in \mathcal{K}\}$ of IoT devices. The joint optimization problem is given by

$$\begin{aligned}
&\underset{\{t_k, p_k, f_k, \Delta_k\}}{\text{maximize}} \quad \min_{k\in\mathcal{K}} \eta_{\text{EE},k} \\
&\text{s.t.} \quad \text{C1: } D_{S,k} + \frac{f_k T}{C_k} \geq D_{k,\min}, \forall k \in \mathcal{K} \\
&\quad \text{C2: } W \log_2\left(1 + \frac{p_k |\mathbf{h}_r^H \Delta_k \mathbf{h}_{I,k} + h_{d,k}|^2}{N_0}\right) - \\
&\quad W \log_2\left(1 + \frac{p_k |\mathbf{g}_r^H \Delta_k \mathbf{h}_{I,k} + g_{d,k}|^2}{N_0}\right) \geq 0, \forall k \in \mathcal{K}, \\
&\quad \text{C3: } \sum_{i=1}^{K} t_i \leq T, \\
&\quad \text{C4: } 0 \leq \phi_{k,m} \leq 2\pi, \forall k \in \mathcal{K}, \forall m \in \mathcal{M}, \\
&\quad \text{C5: } 0 \leq f_k \leq f_{k,\max}, \forall k \in \mathcal{K}, \\
&\quad \text{C6: } 0 \leq p_k \leq P_{k,\max}, \forall k \in \mathcal{K}, \\
&\quad \text{C7: } t_k \geq 0, \forall k \in \mathcal{K},
\end{aligned} \tag{7}$$

where C1 implies that the number of accomplished computation bits at the $k$-th IoT device should be larger than its minimum computation requirement $D_{k,\min}$, C2 indicates that the secure offloading rate should be a positive value, C3 and C7 are time-slot constraints, C4 is the passive beamforming constraint of the RIS, while C5 and C6 restrict the maximum computing frequencies and the maximum transmission power at IoT devices, respectively.

*Remark 1:* Due to the fractional structure of objective function, and the high coupled variables among time, transmit power and phase shift matrix, the problem (7) is a typical non-convex optimization problem, and it is hard to acquire its global optimal solution in polynomial time.

Exploiting the Dinkelbach's method [28], we have the following lemma for transforming the original problem (7) to a more tractable form.

*Lemma 1:* The optimal solution for the computation efficiency maximization problem (7) is achieved if and only if

$$\begin{aligned}
&\underset{\{\Delta_k, t_k, p_k, f_k\}}{\text{maximize}} \min_{k\in\mathcal{K}} D_k(t_k, f_k, p_k, \Delta_k) - u^* E_k(t_k, f_k, p_k) \\
&= \min_{k\in\mathcal{K}} D_k(t_k^*, f_k^*, p_k^*, \Delta_k^*) - u^* E_k(t_k^*, f_k^*, p_k^*) \\
&= 0,
\end{aligned} \tag{8}$$

where $(\cdot)^*$ is the optimal solution, and $u^*$ denotes the achievable maximum computation efficiency of (7).

*Proof:* See Appendix A. ■

However, $u^*$ cannot be obtained in advance, so we adopt an update parameter $u$ to replace $u^*$. Therefore, the optimal solution of (7) can be addressed by alternately solving the following problem:

$$\begin{aligned}
&\underset{\{\Delta_k, t_k, p_k, f_k\}}{\text{maximize}} \min_{k\in\mathcal{K}} D_k - uE_k \\
&\text{s.t.} \quad \text{C1-C7.}
\end{aligned} \tag{9}$$

Next, we introduce an auxiliary variable $\zeta = \min_{k\in\mathcal{K}} D_k - uE_k$ to reformulate (9) as

$$\begin{aligned}
&\underset{\{\Delta_k, t_k, p_k, f_k\}, \zeta}{\text{maximize}} \quad \zeta \\
&\text{s.t.} \quad D_k - uE_k \geq \zeta, \forall k \in \mathcal{K}, \\
&\quad \text{C1-C7.}
\end{aligned} \tag{10}$$

Then, to tackle the coupled optimization variables, we will exploit the classic block coordinate descent technique to transform (10) into four subproblems, namely transmit power control, time-slot allocation, phase beamforming optimization, and local computing frequency optimization subproblems. Moreover, the successive convex approximation (SCA)-based method and penalty function-based algorithm are developed to address the transmit power control and phase beamforming optimization subproblems, respectively, and the closed-form expression for local computing frequencies optimization are derived. The detailed flow chart for solving the original problem (7) is illustrated in Fig. 2.

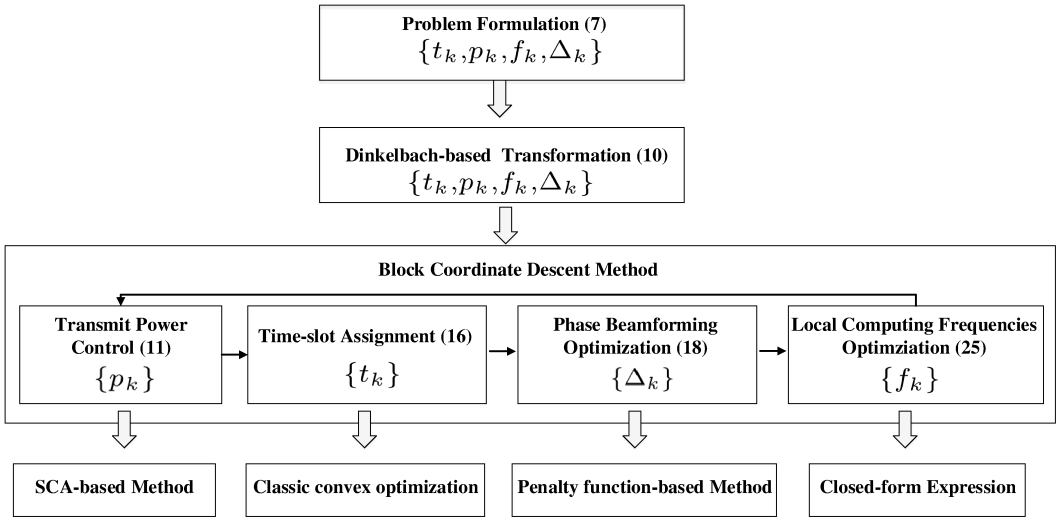


**Fig. 2:** The flow chart of the proposed method

### A. Transmit Power Control

Given $\{\Delta_k^*, t_k^*, f_k^*\}$, (10) reduces to the transmit power control subproblem

$$\underset{\{p_k\},\zeta}{\text{maximize}} \quad \zeta \tag{11a}$$

$$\text{s.t.} \quad D_{O,k}(p_k, t_k^*, \Delta_k^*) - D_{E,k}(p_k, t_k^*, \Delta_k^*) + \frac{f_k^* T}{C_k} - u(p_k t_k^* + \kappa (f_k^*)^3 T) \geq \zeta, \forall k \in \mathcal{K}, \tag{11b}$$

$$D_{O,k}(p_k, t_k^*, \Delta_k^*) - D_{E,k}(p_k, t_k^*, \Delta_k^*) \geq \max\{D_{k,\min} - \frac{f_k^* T}{C_k}, 0\}, \forall k \in \mathcal{K}, \tag{11c}$$

$$\text{C6}, \tag{11d}$$

where

$$D_{O,k}(p_k, t_k^*, \Delta_k^*) = t_k^* W \log_2 \left(1 + \frac{p_k |\mathbf{h}_r^H \Delta_k^* \mathbf{h}_{I,k} + h_{d,k}|^2}{N_0}\right) \tag{12}$$

$$D_{E,k}(p_k, t_k^*, \Delta_k^*) = t_k^* W \log_2 \left(1 + \frac{p_k |\mathbf{g}_r^H \Delta_k^* \mathbf{h}_{I,k} + g_{d,k}|^2}{N_0}\right) \tag{13}$$

It is observed that $D_{S,k}(p_k, t_k^*, \Delta_k^*) = D_{O,k}(p_k, t_k^*, \Delta_k^*) - D_{E,k}(p_k, t_k^*, \Delta_k^*)$ is non-convex and non-concave function, which makes it challenging to obtain the optimal solution of (11). We first express $D_{E,k}(p_k, t_k^*, \Delta_k^*)$ as its first-order Taylor approximation, i.e.,

$$\begin{aligned} & D_{E,k}(p_k, t_k^*, \Delta_k^*) \leq \\ & = D_{E,k}(p_k^{(i)}, t_k^*, \Delta_k^*) + \nabla_{p_k} D_{E,k}(p_k^{(i)}, t_k^*, \Delta_k^*)(p_k - p_k^{(i)}) \\ & = t_k^* W \log_2 \left(1 + \frac{p_k^{(i)} |\mathbf{g}_r^H \Delta_k^* \mathbf{h}_{I,k} + g_{d,k}|^2}{N_0}\right) \\ & + \frac{t_k^* W |\mathbf{g}_r^H \Delta_k^* \mathbf{h}_{I,k} + g_{d,k}|^2}{\log(2)(N_0 + p_k^{(i)} |\mathbf{g}_r^H \Delta_k^* \mathbf{h}_{I,k} + g_{d,k}|^2)} (p_k - p_k^{(i)}) \\ & = \widehat{D_{E,k}}(p_k, t_k^*, \Delta_k^*). \end{aligned} \tag{14}$$

Denoting $D_{E,k}(p_k, t_k^*, \Delta_k^*)$ as $\widehat{D_{E,k}}(p_k, t_k^*, \Delta_k^*)$, the optimal solution of problem (11) is able to be obtained by alternately solving the following problem

$$\underset{\{p_k\},\zeta}{\text{maximize}} \quad \zeta \tag{15a}$$

$$\text{s.t.} \quad D_{O,k}(p_k, t_k^*, \Delta_k^*) - \widehat{D_{E,k}}(p_k, t_k^*, \Delta_k^*) + \frac{f_k^* T}{C_k} - u(p_k t_k^* + \kappa (f_k^*)^3 T) \geq \zeta, \forall k \in \mathcal{K}, \tag{15b}$$

$$D_{O,k}(p_k, t_k^*, \Delta_k^*) - \widehat{D_{E,k}}(p_k, t_k^*, \Delta_k^*) \geq \max\{D_{k,\min} - \frac{f_k^* T}{C_k}, 0\}, \forall k \in \mathcal{K}, \tag{15c}$$

$$\text{C6}, \tag{15d}$$

Based on above descriptions, we establish a SCA-based method to solve the transmit power control subproblem (11), as summarized in Algorithm 1. Furthermore, we prove the convergence of Algorithm 1 in *Theorem 1*.

**Algorithm 1:** SCA-based Method for Solving (11)

1 **Initialize:** Set $(p_1^{(0)}, p_2^{(0)}, \cdots, p_K^{(0)})$, and $i = 1$.
2 **Repeat:**
3 Solve the transformed convex problem (15) by calling CVX to acquire optimal $\{p_k^*\}$;
4 Set $p_k^{(i)} = p_k^*$;
5 Update the iterative number $i = i + 1$;
6 **Until Convergence**.
7 **Obtain** optimal transmit power $\{p_k^{(i)}\}$.

*Theorem 1:* The approximation (14) generates a tight lower bound of $D_{E,k}(p_k, t_k^*, \Delta_k^*)$, and it will further result in a sequence of improved solutions for (15).

*Proof:* See Appendix B. ■

### B. Time-slot Allocation

For given $\{\Delta_k^*, p_k^*, f_k^*\}$, (10) will be transformed to the time-slot assignment subproblem

$$\begin{aligned}
\underset{\{t_k\},\zeta}{\text{maximize}} \quad & \zeta && \text{(16a)}\\
\text{s.t.} \quad & t_k R_{S,k}(p_k^*, \Delta_k^*) + \frac{f_k^* T}{C_k} && \\
& - u(p_k^* t_k + \kappa (f_k^*)^3 T) \geq \zeta, \forall k \in \mathcal{K}, && \text{(16b)}\\
& t_k R_{S,k}(p_k^*, \Delta_k^*) \geq && \\
& \max\{D_{k,\min} - \frac{f_k^* T}{C_k}, 0\}, \forall k \in \mathcal{K}, && \text{(16c)}\\
& \text{C3, C7}, && \text{(16d)}
\end{aligned}$$

where

$$\begin{aligned}
R_{S,k}(p_k^*, \Delta_k^*) =& W \log_2 \left(1 + \frac{p_k^* |\mathbf{h}_r^H \Delta_k^* \mathbf{h}_{I,k} + h_{d,k}|^2}{N_0}\right) - \\
& W \log_2 \left(1 + \frac{p_k^* |\mathbf{g}_r^H \Delta_k^* \mathbf{h}_{I,k} + g_{d,k}|^2}{N_0}\right).
\end{aligned} \tag{17}$$

It is observed that the time-slot assignment subproblem (16) is a linear programming problem, so it can be efficiently solved by interior-point method integrated in convex toolboxes, such as CVX and Yalmip [29], [30].

### C. Phase Beamforming Optimization

Under given $\{p_k^*, t_k^*, f_k^*\}$, (10) reduces the phase beamforming optimization subproblem

$$\begin{aligned}
\underset{\{\Delta_k\},\zeta}{\text{maximize}} \quad & \zeta \\
\text{s.t.} \quad & \text{C8: } t_k^* W \log_2 \left(1 + \frac{p_k^* |\mathbf{h}_r^H \Delta_k \mathbf{h}_{I,k} + h_{d,k}|^2}{N_0}\right) - \\
& t_k^* W \log_2 \left(1 + \frac{p_k^* |\mathbf{g}_r^H \Delta_k \mathbf{h}_{I,k} + g_{d,k}|^2}{N_0}\right) + \\
& \frac{f_k^* T}{C_k} - u(p_k^* t_k^* + \kappa (f_k^*)^3 T) \geq \zeta, \forall k \in \mathcal{K}, \\
& \text{C9: } t_k^* W \log_2 \left(1 + \frac{p_k^* |\mathbf{h}_r^H \Delta_k \mathbf{h}_{I,k} + h_{d,k}|^2}{N_0}\right) - \\
& t_k^* W \log_2 \left(1 + \frac{p_k^* |\mathbf{g}_r^H \Delta_k \mathbf{h}_{I,k} + g_{d,k}|^2}{N_0}\right) \geq \\
& \max\{D_{k,\min} - \frac{f_k^* T}{C_k}, 0\}, \forall k \in \mathcal{K}, \\
& \text{C10: } 0 \leq \phi_{k,m} \leq 2\pi, \forall k \in \mathcal{K}, \forall m \in \mathcal{M}.
\end{aligned} \tag{18}$$

Let us denote $x_k = \frac{p_k^* |\mathbf{h}_r^H \Delta_k \mathbf{h}_{I,k} + h_{d,k}|^2}{N_0}$, $y_k = \frac{p_k^* |\mathbf{g}_r^H \Delta_k \mathbf{h}_{I,k} + g_{d,k}|^2}{N_0}$, $\mathbf{v}_k = [e^{j\phi_{k,1}}, \cdots, e^{j\phi_{k,M}}]^T$, $\hat{\mathbf{v}_k} = [\mathbf{v}_k, 1]^T$, $\mathbf{h}_k^H = [\mathbf{h}_r^H \text{diag}(\mathbf{h}_{I,k}), h_{d,k}]$, and $\mathbf{g}_k^H = [\mathbf{g}_r^H \text{diag}(\mathbf{h}_{I,k}), g_{d,k}]$. Since $|\mathbf{h}_r^H \Delta_k \mathbf{h}_{I,k} + h_{d,k}| = [\mathbf{h}_r^H \text{diag}(\mathbf{h}_{I,k}), h_{d,k}]\hat{\mathbf{v}_k} = \mathbf{h}_k^H \hat{\mathbf{v}_k}$, $|\mathbf{g}_r^H \Delta_k \mathbf{h}_{I,k} + g_{d,k}| = [\mathbf{g}_r^H \text{diag}(\mathbf{h}_{I,k}), g_{d,k}]\hat{\mathbf{v}_k} = \mathbf{g}_k^H \hat{\mathbf{v}_k}$, (18) can be rewritten as the following problem

$$\begin{aligned}
\underset{\{\hat{\mathbf{v}_k}\},\zeta}{\text{maximize}} \quad & \zeta && \text{(19a)}\\
\text{s.t.} \quad & t_k^* W \log_2 (1 + x_k) - t_k^* W \log_2 (1 + y_k) + && \\
& \frac{f_k^* T}{C_k} - u(p_k^* t_k^* + \kappa (f_k^*)^3 T) \geq \zeta, \forall k \in \mathcal{K}, && \text{(19b)}\\
& t_k^* W \log_2 (1 + x_k) - t_k^* W \log_2 (1 + y_k) \geq && \\
& \max\{D_{k,\min} - \frac{f_k^* T}{C_k}, 0\}, \forall k \in \mathcal{K}, && \text{(19c)}\\
& x_k = \frac{p_k^* |\mathbf{h}_k^H \hat{\mathbf{v}_k}|^2}{N_0}, y_k = \frac{p_k^* |\mathbf{g}_k^H \hat{\mathbf{v}_k}|^2}{N_0}, \forall k \in \mathcal{K}, && \text{(19d)}\\
& [\hat{\mathbf{v}_k} \hat{\mathbf{v}_k}^H]_{mm} = 1, \forall k \in \mathcal{K}, \forall m \in \{\mathcal{M}, M+1\}, && \text{(19e)}
\end{aligned}$$

We further introduce a matrix variable $\hat{\mathbf{V}}_k = \hat{\mathbf{v}_k} \hat{\mathbf{v}_k}^H$, and (19) will be converted to the following problem

$$\begin{aligned}
\underset{\{\hat{\mathbf{V}}_k, x_k, y_k\},\zeta}{\text{maximize}} \quad & \zeta && \text{(20a)}\\
\text{s.t.} \quad & x_k = \frac{p_k^* \text{Tr}(\mathbf{H}_k \hat{\mathbf{V}}_k)}{N_0}, y_k = \frac{p_k^* \text{Tr}(\mathbf{G}_k \hat{\mathbf{V}}_k)}{N_0}, \forall k \in \mathcal{K}, && \text{(20b)}\\
& [\hat{\mathbf{V}}_k]_{mm} = 1, \forall k \in \mathcal{K}, \forall m \in \{\mathcal{M}, M+1\}, && \text{(20c)}\\
& \hat{\mathbf{V}}_k \succeq 0, \forall k \in \mathcal{K}, && \text{(20d)}\\
& \text{Rank}(\hat{\mathbf{V}}_k) = 1, \forall k \in \mathcal{K}, && \text{(20e)}\\
& \text{(19b)-(19c)}, && \text{(20f)}
\end{aligned}$$

where $\mathbf{H}_k = \mathbf{h}_k \mathbf{h}_k^H$ and $\mathbf{G}_k = \mathbf{g}_k \mathbf{g}_k^H$. Next, we will handle with the non-convex rank-one constraint (20e). For the positive semi-definite matrix $\hat{\mathbf{V}}_k$, its trace should be no less than its maximum eigenvalue, i.e., $\text{Tr}(\hat{\mathbf{V}}_k) \geq \lambda_{\max}(\hat{\mathbf{V}}_k)$, and the equality holds when $\text{Rank}(\hat{\mathbf{V}}_k) = 1$. Based on this observation, we can add a penalty function $-\sum_{k=1}^{K} (\text{Tr}(\hat{\mathbf{V}}_k) - \lambda_{\max}(\hat{\mathbf{V}}_k))$ in the objective function of (20) and drop the rank-one constraint (20e), to reformulate (20) as

$$\begin{aligned}
\underset{\{\hat{\mathbf{V}}_k, x_k, y_k\},\zeta}{\text{maximize}} \quad & \zeta - \beta \sum_{k=1}^{K} (\text{Tr}(\hat{\mathbf{V}}_k) - \lambda_{\max}(\hat{\mathbf{V}}_k)) && \text{(21a)}\\
\text{s.t.} \quad & \text{(19b)-(19c), (20b)-(20d)} && \text{(21b)}
\end{aligned}$$

where $\beta$ stands for the penalty factor. By rewriting the function $\log_2 (1 + y_k)$ and $\lambda_{\max}(\hat{\mathbf{V}}_k)$ as its first Taylor approximation, the problem (21) will be reformulated as the following convex

problem

$$\underset{\{\hat{\mathbf{V}}_k,x_k,y_k\},\zeta}{\text{maximize}} \quad \zeta-\beta(\sum_{k=1}^{K}\text{Tr}(\hat{\mathbf{V}}_k)-\lambda_{\max}(\hat{\mathbf{V}}_k{}^{(i)}) - (\mathbf{v}_{k,\hat{\max}}{}^{(i)})^H(\hat{\mathbf{V}}_k-\hat{\mathbf{V}}_k{}^{(i)})\mathbf{v}_{k,\hat{\max}}{}^{(i)}) \tag{22a}$$

$$\text{s.t.} \quad t_k^*W\log_2(1+x_k)-(t_k^*W\log_2\left(1+y_k^{(i)}\right)+\frac{t_k^*W(y_k-y_k^{(i)})}{\log(2)(1+y_k^{(i)})})+\frac{f_k^*T}{C_k}-u(p_k^*t_k^*+\kappa(f_k^*)^3T)\geq\zeta,\forall k\in\mathcal{K}, \tag{22b}$$

$$t_k^*W\log_2(1+x_k)-(t_k^*W\log_2\left(1+y_k^{(n)}\right)+\frac{t_k^*W(y_k-y_k^{(n)})}{\log(2)(1+y_k^{(n)})})\geq\max\{D_{k,\min}-\frac{f_k^*T}{C_k},0\},\forall k\in\mathcal{K}, \tag{22c}$$

$$\text{(20b)-(20d)}, \tag{22d}$$

where $\hat{\mathbf{V}}_k{}^{(i)}$ and $y_k^{(i)}$ denote the optimal $\hat{\mathbf{V}}_k$ and $y_k$ in the $i$-th iteration, respectively. By removing the constant terms in (22a), (22) reduces to the following problem

$$\underset{\{\hat{\mathbf{V}}_k,x_k,y_k\},\zeta}{\text{maximize}} \quad \zeta-\beta(\sum_{k=1}^{K}\text{Tr}(\hat{\mathbf{V}}_k)-(\mathbf{v}_{k,\hat{\max}}{}^{(i)})^H\hat{\mathbf{V}}_k\mathbf{v}_{k,\hat{\max}}{}^{(i)}) \tag{23a}$$

$$\text{s.t.} \quad \text{(22b)-(22d)}, \tag{23b}$$

When $\text{Tr}(\hat{\mathbf{V}}_k)-\lambda_{\max}(\hat{\mathbf{V}}_k)\approx 0$, we will have $\hat{\mathbf{V}}_k\approx\lambda_{\max}(\hat{\mathbf{V}}_k)\mathbf{v}_{k,\hat{\max}}\mathbf{v}_{k,\hat{\max}}{}^H$, where $\mathbf{v}_{k,\hat{\max}}$ stands for the unit eigenvector associated with the maximum eigenvalue $\lambda_{\max}(\hat{\mathbf{V}}_k)$. Therefore, the optimal beamforming vector $\mathbf{v}_{k,\hat{\max}}$ can be recovered by the following equation:

$$\hat{\mathbf{v}_k}=\lambda_{\max}(\hat{\mathbf{V}}_k)^{\frac{1}{2}}\mathbf{v}_{k,\hat{\max}}. \tag{24}$$

The detailed method for solving the phase beamfroming optimization problem are given in Algorithm 2. The convergence of the proposed iterative algorithm is proved in *Theorem* 2.

**Algorithm 2:** Penalty function-based Method for Solving (18)

1 **Initialize:** Set $(y_1^{(0)},y_2^{(0)},\cdots,y_K^{(0)})$ and $(\hat{\mathbf{V}}_1{}^{(0)},\hat{\mathbf{V}}_2{}^{(0)},\cdots,\hat{\mathbf{V}}_K{}^{(0)})$ , penalty factor $\beta$, and $i=1$.
2 **Repeat:**
3 Solve the convex optimization problem (23) by calling CVX to obtain optimal $\{\hat{\mathbf{V}}_k{}^*,x_k^*,y_k^*\}$;
4 Set $\hat{\mathbf{V}}_k{}^{(i)}=\hat{\mathbf{V}}_k{}^*$, $y_k^{(i)}=y_k^*$;
5 Update the iterative number $i=i+1$;
6 **Until Convergence**.
7 **Return** optimal phase beamforming matrix $\{\hat{\mathbf{V}}_k{}^{(i)}\}$.

*Theorem 2:* Algorithm 2 improves the objective function value of (23) in each iteration, thus it can coverage to the optimal solution.

*Proof:* The proof is similar to that of *Theorem 1*. ■

### D. Local Computing Frequency Optimization

For given $(t_k^*,p_k^*,\Delta_k^*)$, (10) reduces the local computing frequency optimization problem

$$\underset{\{f_k\},\zeta}{\text{maximize}} \quad \zeta \tag{25a}$$

$$\text{s.t.} \quad D_{S,k}(p_k^*,t_k^*,\Delta_k^*)+\frac{f_kT}{C_k}-u(p_k^*t_k^*+\kappa f_k^3T)\geq\zeta,\forall k\in\mathcal{K}, \tag{25b}$$

$$D_{S,k}(p_k^*,t_k^*,\Delta_k^*)\geq D_{k,\min}-\frac{f_kT}{C_k},\forall k\in\mathcal{K}, \tag{25c}$$

$$\text{C5}, \tag{25d}$$

where

$$D_{S,k}(t_k^*,p_k^*,\Delta_k^*)=t_k^*W\log_2\left(1+\frac{p_k^*|\mathbf{h}_r^H\Delta_k^*\mathbf{h}_{I,k}+h_{d,k}|^2}{N_0}\right)-t_k^*W\log_2\left(1+\frac{p_k^*|\mathbf{g}_r^H\Delta_k^*\mathbf{h}_{I,k}+g_{d,k}|^2}{N_0}\right). \tag{26}$$

Due to the convexity of $f_k^3$ and the linearity of $\frac{f_kT}{C_k}$ with $f_k\geq 0$, thus (25) is a classic convex optimization problem, which can be solved by CVX. In order to gain more insights, we further derive its closed-form solution in following *Theorem 3*.

*Theorem 3:* For given lagrange multipliers $\{\lambda_{1,k},\lambda_{2,k},\lambda_{3,k},k\in\mathcal{K}\}$, the optimal local computing frequency is given by

$$f_k^*=\sqrt{\frac{\frac{\lambda_{1,k}+\lambda_{2,k}}{C_k}-\frac{\lambda_{3,k}}{T}}{3\kappa u\lambda_{1,k}}}. \tag{27}$$

*Proof:* See Appendix C. ■

*Remark 2:*As shown in *Theorem 3*, we observe that the optimal CPU frequency $f_k^*$ decreases with the increase of computational complexity $C_k$. This means that the IoT device tends to offload more high-complexity computation tasks to the AP, in order to improve its computation energy efficiency. Besides, it is observed that a larger time block length $T$ will cause a higher local computing frequency $f_k^*$. It implies that the computation energy efficiency-oriented scheme allows the IoT device to execute more computing tasks via local computing, when the time block length is large.

### E. Overall Algorithm

In order to solve the non-convex non-linear problem (7), we propose an iterative algorithm exploiting the Dinkelbach-based method and block coordinate descent technique. First, we transform the fractional structure of computation efficiency expression to a subtractive formation. Then, we divide the coupled optimization variables into four blocks $\{p_k,t_k,\Delta_k,f_k\}$. The transmit power control $\{p_k\}$, time-slot assignment $\{t_k\}$, phase beamforming $\{\Delta_k\}$, and local computing frequency

$\{f_k\}$ are alternately optimized via solving (11), (16), (18) and (25), respectively, while ensuring the other variables fixed. The detailed procedure for solving (7) is illustrated in the following Algorithm 3.

**Algorithm 3:** Dinkelbach-based method for solving (7)

**Initialize:** set initial $\{u^{(0)}, p_k^{(0)}, t_k^{(0)}, \Delta^{(0)}, f_k^{(0)}\}$, the error tolerance threshold $\epsilon$, and $flag = 0$.
**Repeat:**
  Exploiting Algorithm 1 to obtain optimal transmit power $\{p_k^{(n)}\}$;
  Solving (16) to obtain optimal time-slot assignment $\{t_k^{(n)}\}$;
  Utilizing Algorithm 2 to obtain optimal phase beamforming matrix $\hat{\mathbf{V}}_k{}^{(n)}$;
  Calculating optimal local computing frequencies $\{f_k^{(n)}\}$ via solving (25);
  **if** $(\min\limits_{k\in\mathcal{K}} D_k^{(n)} - u^{(n)} E_k^{(n)}) \leq \epsilon$ **then**
    $(\hat{\mathbf{V}}_k{}^{*}, t_k^*, p_k^*, f_k^*) = (\hat{\mathbf{V}}_k{}^{(n)}, t_k^{(n)}, p_k^{(n)}, f_k^{(n)})$.
    $u^* = \min\limits_{k\in\mathcal{K}} \frac{D_k^{(n)}}{E_k^{(n)}}$ .
    $flag = 1$.
  **else**
    $u^{(n+1)} = \min\limits_{k\in\mathcal{K}} \frac{D_k^{(n)}}{E_k^{(n)}}$.
    $n = n + 1$ .
**Until:** $flag = 1$.

*1) Computational complexity: :* The computational complexity of proposed Algorithm 3 includes two parts, namely the iteration number and the per-iteration complexity. According to [28], the Dinkelbach-type algorithm for max-min fractional optimization problem exhibits a linear convergence rate. We define the iteration number of Algorithm 3 as $Nu_1$. Besides, four subproblems need to be solved in each iteration.

- For the transmit power control subproblem, Algorithm 1 is exploited to solve it. Let $Nu_2$ denote the iteration number of Algorithm 1. Moreover, the interior-point method is utilized to solve (15) in each iteration. Therefore, the computational complexity of Algorithm 1 can be written as $\mathcal{O}(2Nu_2(5K+1)(K+1)^2\sqrt{K}\log(\frac{1}{\epsilon_1}))$ with $K+1$ optimization variables and $4K$ constraints, where $\epsilon_1$ is the tolerance factor.
- For the time-slot assignment and local computing frequencies optimization subproblems, interior-point method is utilized to address them with computational complexity $\mathcal{O}(2(2K+1)(K+1)^2\sqrt{3K+1}\log(\frac{1}{\epsilon_2}))$ and $\mathcal{O}(2(5K+1)(K+1)^2\sqrt{K}\log(\frac{1}{\epsilon_3}))$, respectively.
- For the phase beamforming subproblem, we adopt the Algorithm 2 to solve it. Defining $Nu_3$ as the iteration number, the interior-point method-based solver is emploied to solve it. Therefore, the computational complexity of Algorithm 3 will be $\mathcal{O}(Nu_3(KM^2+2K+1)(KM^2+6K+M+1)\sqrt{4K+M+1}\log(\frac{1}{\epsilon_4}))$

In summary, the complexity of the proposed algorithm for solving (7) can be expressed as $\mathcal{O}(Nu_1(2Nu_2(5K+1)(K+1)^2\sqrt{K}\log(\frac{1}{\epsilon_1}) + 2(2K+1)(K+1)^2\sqrt{3K+1}\log(\frac{1}{\epsilon_2}) + 2(5K+1)(K+1)^2\sqrt{K}\log(\frac{1}{\epsilon_3}) + Nu_3(KM^2+2K+1)(KM^2+6K+M+1)\sqrt{4K+M+1}\log(\frac{1}{\epsilon_4}))$. In particular, we further prove the convergence of Algorithm 3 in the following *Theorem 4*.

*Theorem 4:* The proposed Dinkelbach-type Algorithm 3 can coverage to the optimal solution.

*Proof:* See Appendix D. ■

## IV. Performance Evaluation

This section provides extensive simulation results to evaluate the performance of the proposed RIS-assisted secure task offloading method. In the simulations, the number of IoT devices is set as $K = 2$, and the number of reflection elements is $M = 16$. The coordinations of AP, IoT devices, RIS, and eavesdropper are [0, 0], ([1, 5], [2, 4]), [0, 5] and [4, -4], respectively. The channel model is expressed as Cg= $\gamma_0 d^{-\alpha}\mathbf{g}$, where $\gamma_0 = -30$dB is the path loss at an unit distance, $d$ stands for the distance between wireless communication nodes, $\alpha = 3$ represents the path loss coefficient of communication links, and $\mathbf{g}$ denotes the small-scale fading which follows Rayleigh distribution. In addition, the effective capacitance factor is set as $\kappa = 10^{-27}$, the noise power is $N_0 = 10^{-7}$W, the maximum transmission power and local computing frequencies of IoT devices are set as $p_{k,\max} = 1$ Watt and $f_{k,\max} = 1$ GHZ, respectively. We also plot the following two benchmark methods for performance comparison:

- *Without RIS:* The IoT devices offload their computation tasks to the AP without the aid of RIS, and meanwhile avoiding the information leakage to the eavesdropper.
- *Without eavesdropper:* No eavesdropper exists in the considered RIS-assisted MEC networks.

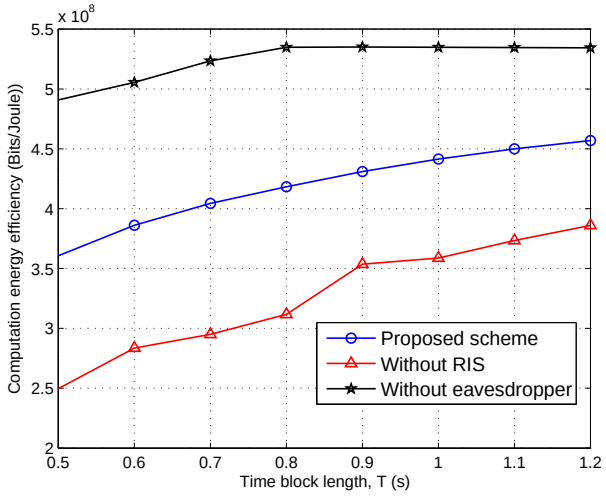


**Fig. 3:** Computation energy efficiency versus time block length

Fig. 3 shows the relationship between the computation efficiency and the time block length, where the computational

complexity is $C_k = 400$ Cycles/bit, the system bandwidth is $W = 5$ MHz, and the minimum computation requirements of IoT devices are set as $D_{k,\min} = 1$ Mbits. It can be seen from Fig. 3 that the computation efficiency of all methods increases with the time block length. This is due to the fact that the IoT devices can decrease their computing frequencies and transmission power for improving the computation efficiency, when the duration of time block is long. In addition, we also observe that the proposed scheme can achieve higher computation efficiency as compared with the counterpart without RIS, especially when the time block length is short. The reason is that the phase shifts of RIS can be adjusted to achieve fine-grained reflect beamforming for improving the secure offloading rate, without consuming more energy. As expected, it reduces the computation efficiency in our proposed method for avoiding the information leakage than the conventional scheme without eavesdroppers.

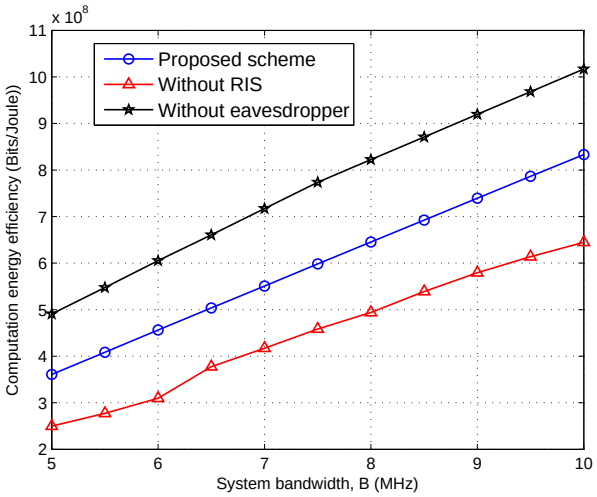


**Fig. 4:** Computation energy efficiency versus system bandwidth

In Fig. 4, we reveal the effect of system bandwidth on the computation efficiency, where the time block length $T = 0.5$ Seconds, $C_k = 400$ Cycles/bit, and $D_{k,\min} = 1$ Mbits. We observe that the computation efficiency of all schemes increases linearly with the system bandwidth. It is easy to understand that a larger system bandwidth implies a higher task offloading rate, and it will further improve the computation efficiency. Moreover, the proposed RIS-assisted secure offloading method can achieve 44.5% higher computation efficiency than the conventional method without the aid of RIS.

Next, Fig. 5 shows the computation efficiency versus the minimum computation requirements of IoT devices, with $T = 0.5$ Seconds, $C_k = 400$ Cycles/bit and $W = 5$ MHz. We see that the computation energy efficiency decreases with the increase in minimum computation requirements of IoT devices. The reason is that the increase of computation requirements may result in more unreasonable energy consumption. In particular, we find that the our proposed method is able to achieve higher performance gain than the baseline method without RIS, when the IoT devices have the heavy computation requirements.

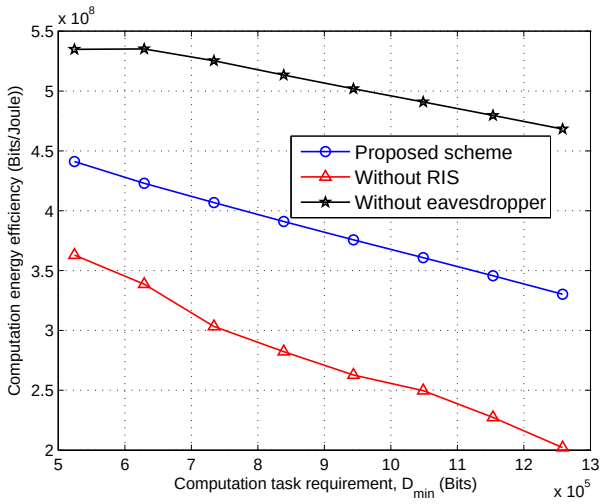


**Fig. 5:** Computation energy efficiency versus computation task requirement

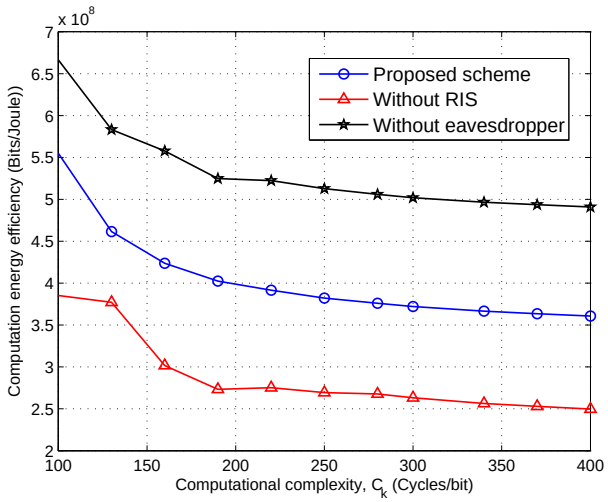


**Fig. 6:** Computation energy efficiency versus computational complexity

Fig. 6 shows the computation efficiency versus the complexity of computation tasks with $T = 0.5$ Seconds, $W = 5$ MHz, and $D_{k,\min} = 1$ Mbits. It is seen from Fig. 6 that the computation efficiency decreases with the increase of computational complexity. Obviously, the higher computational complexity leads to more energy consumption for executing 1-bit task via locally computing, thus it will result in a lower computation energy efficiency. Meanwhile, we also observe that the curve exhibits a inverse ratio relationship with $C_k$, due to the feature of reciprocal function $\frac{f_k T}{C_k}$ in (6).

In Fig 7, we plot the computation efficiency against the path-loss factor of eavesdropping links with $T = 0.5$ Seconds, $W = 5$ MHz, $C_k = 400$ Cycles/bit, and $D_{k,\min} = 1$ Mbits. As shown in Fig. 7, the performance gap between the proposed scheme and the baseline scheme without eavesdroppers decrease with the increase in path-loss factor of eavesdropping links. This is because that the capacity of eavesdropping link

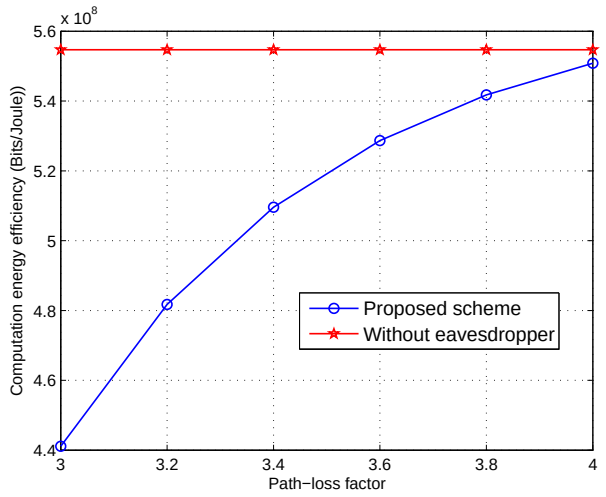


**Fig. 7:** Computation energy efficiency versus path-loss factor

decreases with the increase of path-loss factor, and it will further lead to the increase of both the secure offloading rate and computation efficiency.

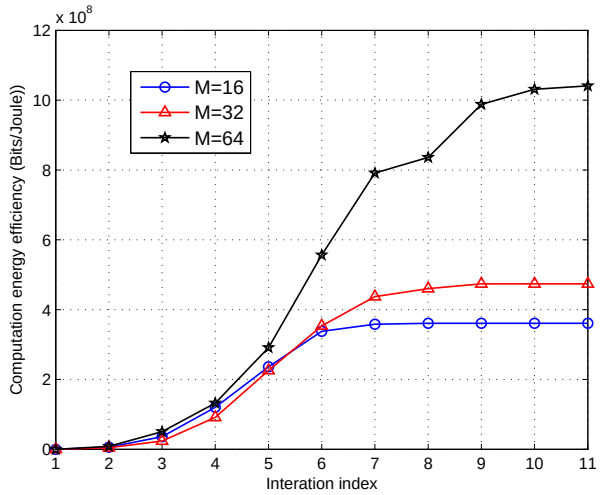


**Fig. 8:** Computation energy efficiency versus iteration index

In Fig. 8, we plot the convergence rate of proposed Algorithm 3 with $T = 0.5$ Seconds, $W = 5$ MHz, $C_k = 400$ Cycles/bit, and $D_{k,\min} = 1$ Mbits. It can be observed that the computation energy efficiency increases very quickly and converges within several iterations. This is because that the Dinkelbach-type algorithm for max-min fractional optimization problem exhibits a linear convergence rate [28]. Specifically, it is also shown that Algorithm 3 exhibits a slower convergence rate when the RIS equips with a larger number of reflection elements. Another important observation is that the system achieves a higher computation energy efficiency when $M$ takes a larger value. This is due to the fact that the additional reflection elements will provide the extra degrees of freedom for designing more efficient phase beamforming strategy.

## V. Conclusion

This paper investigated the secure task offloading and wireless resource management strategy for RIS-enhanced MEC networks. We first formulated a max-min computation energy efficiency problem under IoT devices' secure computation rate constraints. For the purpose of solving the formulated non-convex problem, we developed a Dinkelbach-type algorithm to jointly optimize the local computing frequencies and transmit power of IoT devices, phase beamforming of the RIS, and time-slot assignment. Simulation results validated that our proposed method outperforms the conventional secure offloading scheme without the aid of RIS in terms of computation efficiency. In addition, the proposed secure offloading method can achieve almost the same computation efficiency as compared with the offloading scheme without eavesdroppers, when the path-loss factor of eavesdropping links is large enough.

In the future work, we will investigate the robust secure offloading scheme considering imperfect channel state information of eavesdropping links. Moreover, the artificial noise-assisted method can be further designed to improve the security during the task offloading process. Finally, it is an interesting research topic to extend the current work to the multi-antenna scenario, where the wireless terminals are equipped with multiple antennas for improving the task offloading rate.

## Appendix A: Proof of *Lemma 1*

In this part, we will prove *Lemma 1* according to the sufficient and necessary criteria.

- Sufficient criteria: when the equality (8) holds, we have

$$\begin{aligned} &\min_{k\in\mathcal{K}} D_k(t_k^*, f_k^*, p_k^*, \Delta_k^*) - u^* E_k(t_k^*, f_k^*, p_k^*) = 0, \\ &\min_{k\in\mathcal{K}} D_k(t_k, f_k, p_k, \Delta_k) - u^* E_k(t_k, f_k, p_k) \le 0. \end{aligned} \tag{28}$$

  At that point, we can derive that

$$\begin{aligned} &\min_{k\in\mathcal{K}} \frac{D_k(t_k^*, f_k^*, p_k^*, \Delta_k^*)}{E_k(t_k^*, f_k^*, p_k^*)} = u^*, \\ &\min_{k\in\mathcal{K}} \frac{D_k(t_k, f_k, p_k, \Delta_k)}{E_k(t_k, f_k, p_k)} \le u^*, \end{aligned} \tag{29}$$

  Thus, $(t_k^*, f_k^*, p_k^*, \Delta_k^*)$ is the optimal solution of original problem (7).
- Necessary criteria: when $(t_k^*, f_k^*, p_k^*, \Delta_k^*)$ is optimal solution of problem (7), we have

$$\min_{k\in\mathcal{K}} \frac{D_k(t_k^*, f_k^*, p_k^*, \Delta_k^*)}{E_k(t_k^*, f_k^*, p_k^*)} = u^*, \tag{30}$$

  After some simple transformation, we can conclude that

$$\min_{k\in\mathcal{K}} D_k(t_k^*, f_k^*, p_k^*, \Delta_k^*) - u^* E_k(t_k^*, f_k^*, p_k^*) = 0, \tag{31}$$

  Based on above derivation, we completes this proof.

## Appendix B: Proof of *Theorem 1*

As $D_{E,k}(p_k, t_k^*, \Delta_k^*)$ is a concave function, it follows that

$$D_{E,k}(p_k, t_k^*, \Delta_k^*) \le \widehat{D_{E,k}}(p_k, t_k^*, \Delta_k^*). \tag{32}$$

Then, we have

$$\begin{aligned} &D_{O,k}(p_k^{(i+1)}, t_k^*, \Delta_k^*) - D_{E,k}(p_k^{(i+1)}, t_k^*, \Delta_k^*) \overset{(a1)}{\geq} \\ &D_{O,k}(p_k^{(i+1)}, t_k^*, \Delta_k^*) + D_{E,k}(p_k^{(i+1)}, t_k^*, \Delta_k^*) \\ &+ \nabla_{p_k} D_{E,k}(p_k^{(i+1)}, t_k^*, \Delta_k^*)(p_k^{(i+1)} - p_k^{(i)}) \\ &\overset{(a2)}{\geq} D_{O,k}(p_k^{(i)}, t_k^*, \Delta_k^*) + D_{E,k}(p_k^{(i)}, t_k^*, \Delta_k^*) + \\ &\nabla_{p_k} D_{E,k}(p_k^{(i)}, t_k^*, \Delta_k^*)(p_k^{(i)} - p_k^{(i)}) = \\ &D_{O,k}(p_k^{(i)}, t_k^*, \Delta_k^*) - D_{E,k}(p_k^{(i)}, t_k^*, \Delta_k^*), \end{aligned} \tag{33}$$

where $(a1)$ holds since the concave function $D_{E,k}(p_k, t_k^*, \Delta_k^*)$ should be less than its first-order Taylor approximation, $(a2)$ holds because for given $p_k^{(i)}$, $p_k^{(i+1)}$ is the optimal solution for (15) at the $(k+1)$-th iteration. Therefore, $p_k^{(i+1)}$ is always better than $p_k^{(i)}$. Integrating with the compactness of feasible set, the sequence $p_k^{(i)}$ can always converges according to the Cauchy theorem.

## Appendix C: Proof of *Theorem 2*

The Lagrange function of (25) will be

$$\begin{aligned} L(f_k, \lambda_{1,k}, \lambda_{2,k}, \lambda_{3,k}) &= -\zeta + \sum_{k=1}^{K} \lambda_{1,k}(\zeta + u(p_k^* + \kappa(f_k)^3 T) \\ &- D_{S,k}(p_k^*, t_k^*, \Delta_k^*) - \frac{f_k T}{C_k}) + \sum_{k=1}^{K} \lambda_{2,k}(D_{k,\min} \\ &- D_{S,k}(p_k^*, t_k^*, \Delta_k^*) - \frac{f_k T}{C_k}) + \sum_{k=1}^{K} \lambda_{3,k}(f_k - f_{k,\max}). \end{aligned} \tag{34}$$

Taking the partial derivative of $L(f_k, \zeta, \lambda_{1,k}, \lambda_{2,k}, \lambda_{3,k})$ to $f_k$, we have

$$\frac{\partial L}{\partial f_k} = 3\lambda_{1,k} u \kappa T (f_k)^2 - \frac{\lambda_{1,k} T}{C_k} - \frac{\lambda_{2,k} T}{C_k} + \lambda_{3,k}. \tag{35}$$

By letting $\frac{\partial L}{\partial f_k} = 0$, we can derive the optimal local computing frequency $f_k^*$ as illustrated in (27).

## Appendix D: Proof of *Theorem 3*

Given the optimal $\mathbf{x}^{(n)} = \{p_k^{(n)}, t_k^{(n)}, \hat{\mathbf{V}}_k^{(n)}, f_k^{(n)}\}$ in $n$-th iteration and $u^{(n+1)} = \min_{k \in \mathcal{K}} \frac{D_k(\mathbf{x}^{(n)})}{E_k(\mathbf{x}^{(n)})}$, it follows that

$$\begin{aligned} \zeta(\mathbf{x}^{(n)}) &= \min\nolimits_{k \in \mathcal{K}} D_k(\mathbf{x}^{(n)}) - u^{(n)} E_k(\mathbf{x}^{(n)}) \\ &\leq \min\nolimits_{k \in \mathcal{K}} (u^{(n+1)} - u^{(n)}) E_k(\mathbf{x}^{(n)}). \end{aligned} \tag{36}$$

Due to the non-negative of $\zeta(\mathbf{x}^{(n)})$ and $E_k(\mathbf{x}^{(n)})$, we have

$$u^{(n+1)} - u^{(n)} \geq 0. \tag{37}$$

Therefore, $u$ is non-decreasing with the iteration index $n$ in Algorithm 3. Combined with the boundedness of maximum computation energy efficiency, we can deduce that Algorithm 3 can coverage to an optimal solution.

## References


[1] Y. Mao, C. You, J. Zhang, K. Huang, and K. B. Letaief, "A survey on mobile edge computing: The communication perspective," *IEEE Communications Surveys and Tutorials*, vol. 19, no. 4, pp. 2322–2358, Fourth Quarter. 2017.

[2] N. Abbas, Y. Zhang, A. Taherkordi, and T. Skeie, "Mobile edge computing: A survey," *IEEE Internet of Things Journal*, vol. 5, no. 1, pp. 450–465, Feb. 2018.

[3] S. Mao, S. Leng, S. Maharjan, and Y. Zhang, "Energy efficiency and delay tradeoff for wireless powered mobile-edge computing systems with multi-access schemes," *IEEE Transactions on Wireless Communications*, vol. 19, no. 3, pp. 1855–1867, Mar. 2020.

[4] X. Hu, K. Wong, and K. Yang, "Wireless powered cooperation-assisted mobile edge computing," *IEEE Transactions on Wireless Communications*, vol. 17, no. 4, pp. 2375–2388, Apr. 2018.

[5] X. He, R. Jin, and H. Dai, "Physical-layer assisted secure offloading in mobile-edge computing," *IEEE Transactions on Wireless Communications*, vol. 19, no. 6, pp. 4054–4066, Jun. 2020.

[6] J. Xu and J. Yao, "Exploiting physical-layer security for multiuser multicarrier computation offloading," *IEEE Wireless Communications Letters*, vol. 8, no. 1, pp. 9–12, Feb. 2019.

[7] Q. Wu and R. Zhang, "Intelligent reflecting surface enhanced wireless network via joint active and passive beamforming," *IEEE Transactions on Wireless Communications*, vol. 18, no. 11, pp. 5394–5409, Nov. 2019.

[8] C. Huang, A. Zappone, G. C. Alexandropoulos, M. Debbah, and C. Yuen, "Reconfigurable intelligent surfaces for energy efficiency in wireless communication," *IEEE Transactions on Wireless Communications*, vol. 18, no. 8, pp. 4157–4170, Aug. 2019.

[9] Q. Wu and R. Zhang, "Towards smart and reconfigurable environment: Intelligent reflecting surface aided wireless network," *IEEE Communications Magazine*, vol. 58, no. 1, pp. 106–112, Jan. 2020.

[10] ——, "Joint active and passive beamforming optimization for intelligent reflecting surface assisted SWIPT under QoS constraints," *IEEE Journal on Selected Areas in Communications*, vol. 38, no. 8, pp. 1735–1748, Aug. 2020.

[11] S. Mao, S. Leng, K. Yang, X. Huang, and Q. Zhao, "Fair energy-efficient scheduling in wireless powered full-duplex mobile-edge computing systems," in *GLOBECOM 2017 - 2017 IEEE Global Communications Conference*, 2017, pp. 1–6.

[12] F. Zhou and R. Q. Hu, "Computation efficiency maximization in wireless-powered mobile edge computing networks," *IEEE Transactions on Wireless Communications*, vol. 19, no. 5, pp. 3170–3184, May. 2020.

[13] S. Bi and Y. J. Zhang, "Computation rate maximization for wireless powered mobile-edge computing with binary computation offloading," *IEEE Transactions on Wireless Communications*, vol. 17, no. 6, pp. 4177–4190, Sept. 2018.

[14] L. Huang, S. Bi, and Y.-J. A. Zhang, "Deep reinforcement learning for online computation offloading in wireless powered mobile-edge computing networks," *IEEE Transactions on Mobile Computing*, vol. 19, no. 11, pp. 2581–2593, Nov. 2020.

[15] C. You, K. Huang, H. Chae, and B. Kim, "Energy-efficient resource allocation for mobile-edge computation offloading," *IEEE Transactions on Wireless Communications*, vol. 16, no. 3, pp. 1397–1411, Mar. 2017.

[16] Z. Ding, J. Xu, O. A. Dobre, and H. V. Poor, "Joint power and time allocation for NOMAMEC offloading," *IEEE Transactions on Vehicular Technology*, vol. 68, no. 6, pp. 6207–6211, Jun. 2019.

[17] T. Bai, C. Pan, Y. Deng, M. Elkashlan, A. Nallanathan, and L. Hanzo, "Latency minimization for intelligent reflecting surface aided mobile edge computing," *IEEE Journal on Selected Areas in Communications*, vol. 38, no. 11, pp. 2666–2682, 2020.

[18] S. Mao, J. Wu, L. Liu, D. Lan, and A. Taherkordi, "Energy-efficient cooperative communication and computation for wireless powered mobile-edge computing," *IEEE Systems Journal*, pp. 1–12, 2020, doi=10.1109/JSYST.2020.3020474.

[19] J.-B. Wang, H. Yang, M. Cheng, J.-Y. Wang, M. Lin, and J. Wang, "Joint optimization of offloading and resources allocation in secure mobile edge computing systems," *IEEE Transactions on Vehicular Technology*, vol. 69, no. 8, pp. 8843–8854, Aug. 2020.

[20] T. Bai, J. Wang, Y. Ren, and L. Hanzo, "Energy-efficient computation offloading for secure UAV-edge-computing systems," *IEEE Transactions on Vehicular Technology*, vol. 68, no. 6, pp. 6074–6087, Jun. 2019.

[21] W. Wu, F. Zhou, R. Q. Hu, and B. Wang, "Energy-efficient resource allocation for secure NOMA-enabled mobile edge computing networks," *IEEE Transactions on Communications*, vol. 68, no. 1, pp. 493–505, Jan. 2020.

[22] J. Chen, Y.-C. Liang, Y. Pei, and H. Guo, "Intelligent reflecting surface: A programmable wireless environment for physical layer security," *IEEE Access*, vol. 7, pp. 82 599–82 612, Jun. 2019.

[23] S. Hong, C. Pan, H. Ren, K. Wang, and A. Nallanathan, "Artificial-noise-aided secure mimo wireless communications via intelligent re-

flecting surface," *IEEE Transactions on Communications*, vol. 68, no. 12, pp. 7851–7866, Dec. 2020.

[24] X. Yu, D. Xu, Y. Sun, D. W. K. Ng, and R. Schober, "Robust and secure wireless communications via intelligent reflecting surfaces," *IEEE Journal on Selected Areas in Communications*, vol. 38, no. 11, pp. 2637–2652, Nov. 2020.

[25] S. Xu, J. Liu, and Y. Cao, "Intelligent reflecting surface empowered physical layer security: Signal cancellation or jamming?" *IEEE Internet of Things Journal*, pp. 1–1, 2021.

[26] H. Sun, F. Zhou, and R. Q. Hu, "Joint offloading and computation energy efficiency maximization in a mobile edge computing system," *IEEE Transactions on Vehicular Technology*, vol. 68, no. 3, pp. 3052–3056, Mar. 2019.

[27] J. Zhang, L. Zhou, F. Zhou, B.-C. Seet, H. Zhang, Z. Cai, and J. Wei, "Computation-efficient offloading and trajectory scheduling for multi-UAV assisted mobile edge computing," *IEEE Transactions on Vehicular Technology*, vol. 69, no. 2, pp. 2114–2125, Feb. 2020.

[28] A. Zappone and E. Jorswieck, "Energy efficiency in wireless networks via fractional programming theory," *Foundations and Trends in Communications and Information Theory*, vol. 11, no. 3-4, pp. 185–396, 2015.

[29] M. Grant and S. Boyd, "CVX: Matlab software for disciplined convex programming, version 2.1," 2014.

[30] J. Lofberg, "YALMIP: A toolbox for modeling and optimization in matlab," in *2004 IEEE international conference on robotics and automation (IEEE Cat. No. 04CH37508)*, 2004, pp. 284–289.